Particle Transport in Magnetophoretic Microsystems

E. P. Furlani

The Institute for Lasers, Photonics, and Biophotonics, University at Buffalo SUNY
432 Natural Science Complex
Buffalo, NY 14260-3000
efurlani@buffalo.edu

ABSTRACT

We present methods and models for predicting the transport and trapping of magnetic particles in microfluidic systems with magnetic functionality. We discuss particle transport models that take into account the dominant magnetic and fluidic forces, as well as Brownian motion for sufficiently small particles. We use the transport models to study the performance of magnetically-biased and electrically actuated microsystems.

Keywords: magnetophoresis, magnetically biased microsystem, micro total analysis system (μTAS), magnetic bioseparation, magnetophoretic microsystem, Lab-on-Chip.

1 INTRODUCTION

Magnetophoresis involves the manipulation of colloidal magnetic particles using an applied magnetic field. The interest in this phenomenon has grown dramatically in recent years, especially for microscale applications in fields such as microbiology and biotechnology where magnetic particles are used to selectively label a target biomaterial to facilitate analysis. This interest has led to the development of magnetophoretic microsystems for applications such as bioseparation and bioassays that involve the separation, sorting or immobilization of a target biomaterial [1]. The ability to magnetically label and manipulate biomaterials such as proteins, enzymes, nucleic acids and whole cells at the microscale enables rapid and highly specific detection and characterization of such materials. The development of magnetophoretic microsystems is progressing rapidly due to advances in microfluidics, especially with regards to on-chip integration of electronic, optical and magnetic functionality, as well as the development of biofunctional magnetic particles that can selectively label a target biomaterial.

In their most basic form magnetophoretic microsystems consist of a microchannel and embedded elements that produce a magnetic field distribution within the microchannel. The elements can be either passive magnetic structures, or active voltage-driven conductors [2-4]. In either case, the field generated by the elements gives rise to a magnetic force that acts to manipulate or trap particles as they flow through the microchannel. Magnetophoretic microsystems are well suited for bioapplications because they enable (i) fast reaction times, (ii) efficient coupling between the applied field and magnetically labeled material, (iii) the analysis and monitoring of small samples (pico/nano-liters), and (iv) the integration of "micro total analysis systems" (μTAS).

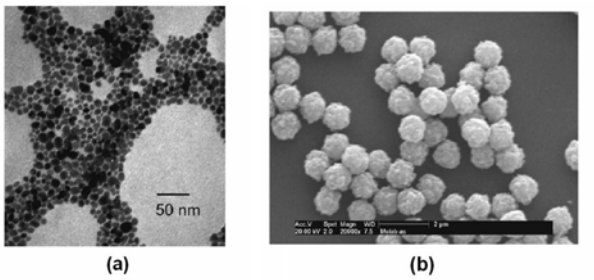

Figure 1: Magnetic particles: (a) TEM of Fe_3O_4 nanoparticles, and (b) polymeric microparticles with embedded magnetic nanoparticles (Dynabeads from Dynal Biotech).

The development of magnetophoretic microsystems requires substantial upfront modeling in order to assess design feasibility, and to optimize performance prior to fabrication. Methods for modeling such devices include coupled magnetic/fluidic numerical analysis as well as analytical techniques if the devices have relatively simple flow geometries and magnetic structures. In this presentation we discuss methods and models for predicting the transport and trapping of magnetic particles in magnetophoretic microsystems. We discuss two different transport models: a classical Newtonian model for predicting the motion of individual particles, and a drift-diffusion model for predicting the behavior of a concentration of nanoparticles, which accounts for the effects of Brownian motion. We also describe a magnetization model for predicting the magnetic response of a particle in an external field that takes into account saturation. This model is needed to compute the force on the particle. We use the transport models to study and compare magnetically-biased and electrically actuated (current driven) microsystems.

2 PARTICE TRANSPORT

Particle transport in a magnetophoretic microsystem is governed by various factors including (a) the magnetic force due to all field sources, (b) the fluidic drag force , (c) inertia, (d) gravity, (e) buoyancy, (f) Brownian motion (g) particle/fluid interactions (perturbations to the flow field), and (h) interparticle effects such as (i) magnetic dipole interactions, (ii) electric double-layer interactions, and (iii) van der Walls force [2-4]. We consider applications involving submicron particles in a dilute suspension where interparticle effects are negligible, and the magnetic and viscous forces are dominant. We present two different models for predicting particle transport in such systems, each governing a different regime of transport (Fig. 2). In the first model, we neglect Brownian motion and use classical Newtonian physics to predict the motion of individual particles, submicron-sized or larger. In the second model, we account for Brownian motion by solving a drift-diffusion equation for the behavior of a concentration of non-interacting magnetic nanoparticles.

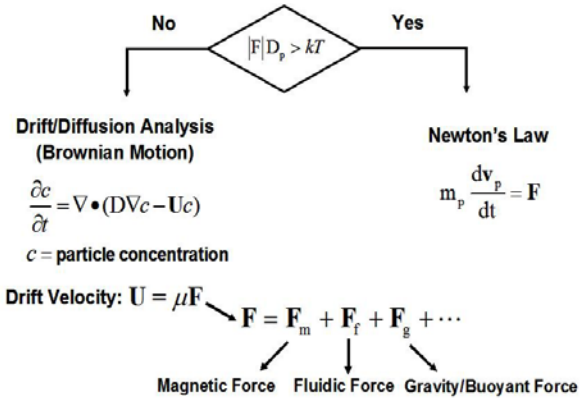

Figure 2: Magnetic particle transport models.

2.1 Newtonian Transport

We consider the motion of a spherical magnetic particle in a viscous carrier fluid under the influence of an applied field. We restrict our attention to slow flow regimes where the magnetic and viscous drag forces are dominant, and we neglect Brownian motion. The particle has a density ρ_p, radius R_p, volume $V_p = \frac{4}{3}\pi R_p^3$, and mass $m_p = \rho_p V_p$. We use classical Newtonian dynamics to study particle motion,

$$m_p \frac{d\mathbf{v}_p}{dt} = \mathbf{F}_m + \mathbf{F}_f + \mathbf{F}_g, \qquad (1)$$

where $\mathbf{v}_p$ is the velocity of the particle, and $\mathbf{F}_m$, $\mathbf{F}_f$, and $\mathbf{F}_g$ are the magnetic, fluidic, and gravitational forces, respectively.

We model the magnetic force using an "effective" dipole moment approach wherein the magnetized particle is replaced by an "equivalent" point dipole [2]. The magnetic force on the dipole (and hence on the particle) is given by,

$$\mathbf{F}_m = \mu_f \left(\mathbf{m}_{p,eff} \bullet \nabla\right)\mathbf{H}_a, \qquad (2)$$

where μ_f is the permeability of the transport fluid, $\mathbf{m}_{p,eff}$ is the "effective" dipole moment of the particle, and $\mathbf{H}_a$ is the applied magnetic field intensity at the center of the particle, were the equivalent point dipole is located. Thus, to predict the magnetic force we need (i) a model for the magnetic response of the particle, from which we obtain $\mathbf{m}_{p,eff}$, and (ii) an expression for the applied field. A model has been developed for $\mathbf{m}_{p,eff}$ that takes into account magnetic saturation of the particle [2]. Specifically, $\mathbf{m}_{p,eff} = V_p f(H_a)\mathbf{H}_a$ where

$$f(H_a) = \begin{cases} \dfrac{3(\chi_p - \chi_f)}{(\chi_p - \chi_f) + 3} & H_a < \left(\dfrac{(\chi_p - \chi_f) + 3}{3(\chi_p - \chi_f)}\right) M_{sp} \\ M_{sp} / H_a & H_a \geq \left(\dfrac{(\chi_p - \chi_f) + 3}{3(\chi_p - \chi_f)}\right) M_{sp} \end{cases}, \qquad (3)$$

M_{sp} is the saturation magnetization of the particle and $H_a = |\mathbf{H}_a|$. Analytical expressions for the field distributions of common magnetic sources (e.g., rectangular magnetic structures and current carrying conductors) can be found in the literature [2-4].

The fluidic force is obtained using Stokes' law for the viscous drag on a sphere,

$$\mathbf{F}_f = -6\pi\eta R_{hyd,p}(\mathbf{v}_p - \mathbf{v}_f), \qquad (4)$$

where $R_{hyd,p}$ is the effective hydrodynamic radius of the particle, and η and $\mathbf{v}_f$ are the viscosity and the velocity of the fluid, respectively. It is important to note that $R_{hyd,p}$ is greater than the physical radius of the particle as surface-bound materials contribute to the viscous drag.

The gravitational force takes into account buoyancy and is given by

$$F_g = -V_p(\rho_p - \rho_f)g \qquad (5)$$

where ρ_p and ρ_f are the densities of the particle and fluid, respectively, and $g = 9.8\ m/s^2$ is the acceleration due to gravity. The inertial term $m_p \frac{d\mathbf{v}_p}{dt}$ in Eq. (1) is often

NSTI-Nanotech 2009, www.nsti.org, ISBN 978-1-4398-1784-1 Vol. 3, 2009

negligible. If we substitute Eq. (4) into Eq. (1) and ignore this term we obtain

$$\frac{dx_p}{dt} = \mathbf{v}_\mathrm{f} + \gamma\left(\mathbf{F}_\mathrm{m} + \mathbf{F}_\mathrm{g}\right), \qquad (6)$$

where $\gamma = 1/(6\pi\eta \mathrm{R}_{hyd,\mathrm{p}})$ is the mobility of the particle. We use Eqs. (1) or (6) to predict the motion of a biofunctional particle given appropriate initial conditions. Oftentimes, the gravitational force $\mathbf{F}_\mathrm{g}$ is also negligible, which further simplifies the analysis.

2.2 Drift-Diffusion Transport

As noted above, Eq. (1) does not take into account Brownian motion, which can influence particle motion when the particle diameter D_p is sufficiently small. We estimate this diameter using the following criterion [3]

$$\left|\mathrm{F}\right|\mathrm{D}_\mathrm{p} \le k\mathrm{T}, \qquad (7)$$

where $\left|\mathrm{F}\right|$ is the magnitude of the applied force acting on the particle. This condition implies that Brownian motion needs to be taken into account when the energy exerted by the applied force in moving the particle a distance equal to its diameter is less than or comparable to thermal energy kT. In order to apply Eq. (7), one needs to estimate $\left|\mathrm{F}\right|$. If a field source is specified, and the magnetic force is the dominant force, then one can estimate $\left|\mathrm{F}\right|$ for a given particle over the region of interest. This can be used to estimate the critical particle diameter $D_{c,p}$ below which one solves a drift-diffusion equation for the particle volume concentration c, rather than the Newtonian equation for the trajectory of a single particle. Specifically, c is governed by the following equation [2],

$$\frac{\partial c}{\partial t} + \nabla \bullet \mathbf{J} = 0, \qquad (8)$$

where $\mathbf{J} = \mathbf{J}_D + \mathbf{J}_A$ is the total flux of particles, which includes a contribution $\mathbf{J}_D = -D\nabla c$ due to diffusion, and a contribution $\mathbf{J}_A = \mathbf{U}c$ due to the drift of the particles under the influence of applied forces. The diffusion coefficient D is given by the Nernst-Einstein relation $D = \gamma kT$. The drift velocity $\mathbf{U}$ in $\mathbf{J}_A$ is obtained in the limit of negligible inertia as in Eq. (6), i.e. $\mathbf{U} = \gamma\mathbf{F}$, where $\mathbf{F} = \frac{\mathbf{v}_\mathrm{f}}{\gamma} + \mathbf{F}_\mathrm{m} + \mathbf{F}_\mathrm{g}$. Note that if the Stokes' drag is the only force, then $\mathbf{U} = \mathbf{v}_\mathrm{f}$.

3 MAGETOPHORETIC MICROSYSTEMS

We use the transport models to study and compare passive (magnetically-biased) and active (voltage activated) microsystems. We study idealized systems. The passive microsystem, shown in Fig. 3, consists of an array of integrated soft-magnetic (permalloy) elements embedded in a nonmagnetic substrate beneath a microfluidic channel. A bias field of 0.5 T is used to magnetize/saturate the elements. A hypothetical separation sequence for this system is depicted in a cross-sectional view in Fig. 3(IV).
The active microsystem, shown in Fig. 4, consists of a parallel array of rectangular conductive elements embedded beneath a microfluidic channel. The dimensions of the microchannel and the elements are the same in both microsystems. Specifically, the microchannel is 120μm high, and each element is 100 μm wide and 50 μm high. The elements are spaced 100 μm apart edge-to-edge. Each conductive element carries a current of I = 450 mA, which corresponds to a current density of $\mathrm{J} = 9\times10^7$ A/m^2. The direction of current alternates from conductor to conductor.

We compute the magnetic force on a 100 nm Fe_3O_4 particle (R_p = 50 nm, $\mathrm{M}_{sp} = 4.78\times10^5$ A/m) in the microchannel above an array of three elements.

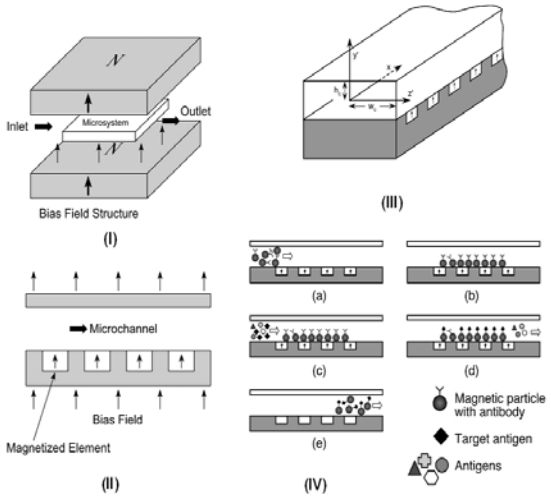

Figure 3: Magnetically-biased microsystem [2]: (I) microsystem with bias field structure, (II) cross section showing microchannel, (III) geometry/reference frame, and (IV) cross-section of microsystem illustrating bioseparation sequence: (a) magnetic particles with surface-bound antibodies enter the microchannel with the bias field applied and the elements magnetized, (b) magnetized elements capture the particles, (c) target antigens are introduced into the microchannel, (d) target antigens become immobilized on captured magnetic particles, (e) the bias field is removed and the magnetic elements revert to an unmagnetized state releasing the separated material for further processing.

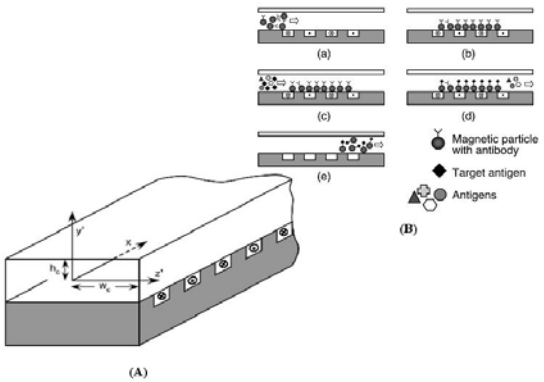

Figure 4: Active microsystem [3]: (A) perspective view with reference frame, (B) cross-section illustrating bioseparation sequence.

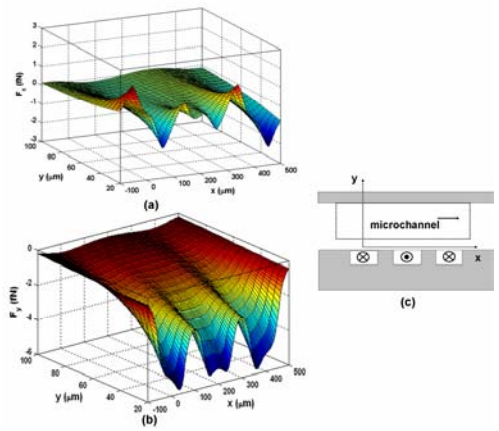

Figure 5: Magnetic force across the microchannel above three conductors: (a) surface plot of F_{mx}, (b) surface plot of F_{my}., (c) area (dotted line) over which the magnetic force is computed.

The force components F_{mx} and F_{my} for the active and passive elements are shown in Figs. 5 and 6, respectively. These are computed over the dotted rectangular region show in Figs. 5c and 6c, which extends from 20 μm to 100 μm above the elements, and from -100 μm to the left of the array to + 100 μm to the right of the array. Note that the magnetized elements produce pico-Newton forces, but the active elements produce only sub-femto-Newton forces. Moreover, while the force profiles of F_{mx} are similar, the profiles for F_{my}, which acts to trap the particles, are different., i.e. this force can be attractive or repulsive for the passive elements with a bias field, but it is strictly attractive for the conductive elements. Typical predicted trajectories of the particles in the passive microsystem are shown in Fig. 7.

4 CONCLUSIONS

The development of microfluidic devices with magnetic functionality is in its infancy and growing rapidly,

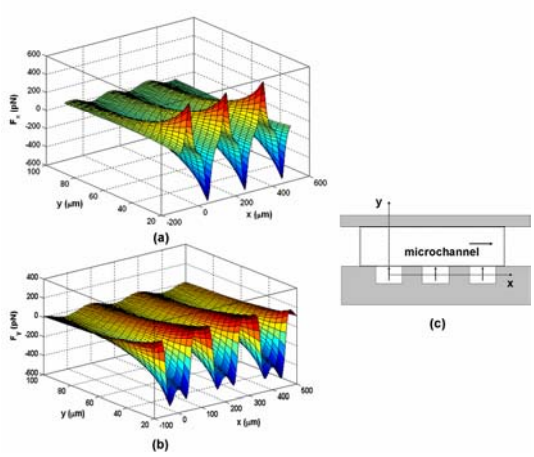

Figure 6: Magnetic force across the microchannel above three magnetized elements: (a) surface plot of F_{mx}, (b) surface plot of F_{my}., (c) area (dotted line) over which the magnetic force is computed.

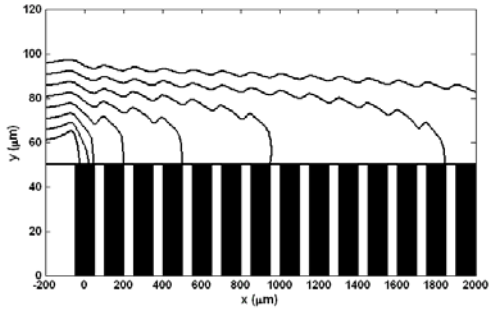

Figure 7: Trajectories of nanoparticles.

especially for bioapplications. Magnetophoretic microsystems utilize either passive or active force generation. Passive systems can provide a much stronger magnetic force than voltage-driven systems, and are more appropriate for nanoparticle transport. Active systems enable more control of the force and are more appropriate for applications that use larger (micron-sized) particles (beads).

REFERENCES

[1] S. Hardt and F. Schönfeld. (eds.), *Microfluidic technologies for miniaturized analysis system*. Springer, New York, 2007.

[2] E. P. Furlani, "Analysis of Particle Transport in a Magnetophoretic Microsystem," J. Appl. Phys. **99**, 2006.

[3] E. P. Furlani , Y. Sahoo , K. C. Ng, J. C. Wortman and T. E. Monk, "A Model for Predicting Magnetic Particle Capture in a Microfluidic Bioseparator," Biomedical Microdevices, **9**, 451-463, 2007.

[4] E. P. Furlani, "Magnetophoretic Separation of Blood Cells at the Microscale," J. Phys. D: Appl. Phys**. 40** 1313-1319, 2007**.**